Electronic Supplementary Information:

"Unraveling the effect of reagent vibrational excitation on the scattering mechanism of the benchmark, H + H_2 → H_2 + H, hydrogen exchange reaction on the coupled $1^2E'$ ground electronic manifold"

Jayakrushna Sahoo,[1, a)] Sugata Goswami,[1, b)] and S. Mahapatra[1, c)]

School of Chemistry, University of Hyderabad, Hyderabad, 500 046, India

[a)]Present address: Laboratoire Univers et Particules de Montpellier, Université de Montpellier, UMR-CNRS 5299, 34095 Montpellier Cedex, France

[b)]Present address: Department of Chemistry, Medi-Caps University, A.B. Road, Pigdamber, Indore - 453 331 (M.P.), India

[c)]Electronic mail: susanta.mahapatra@uohyd.ac.in

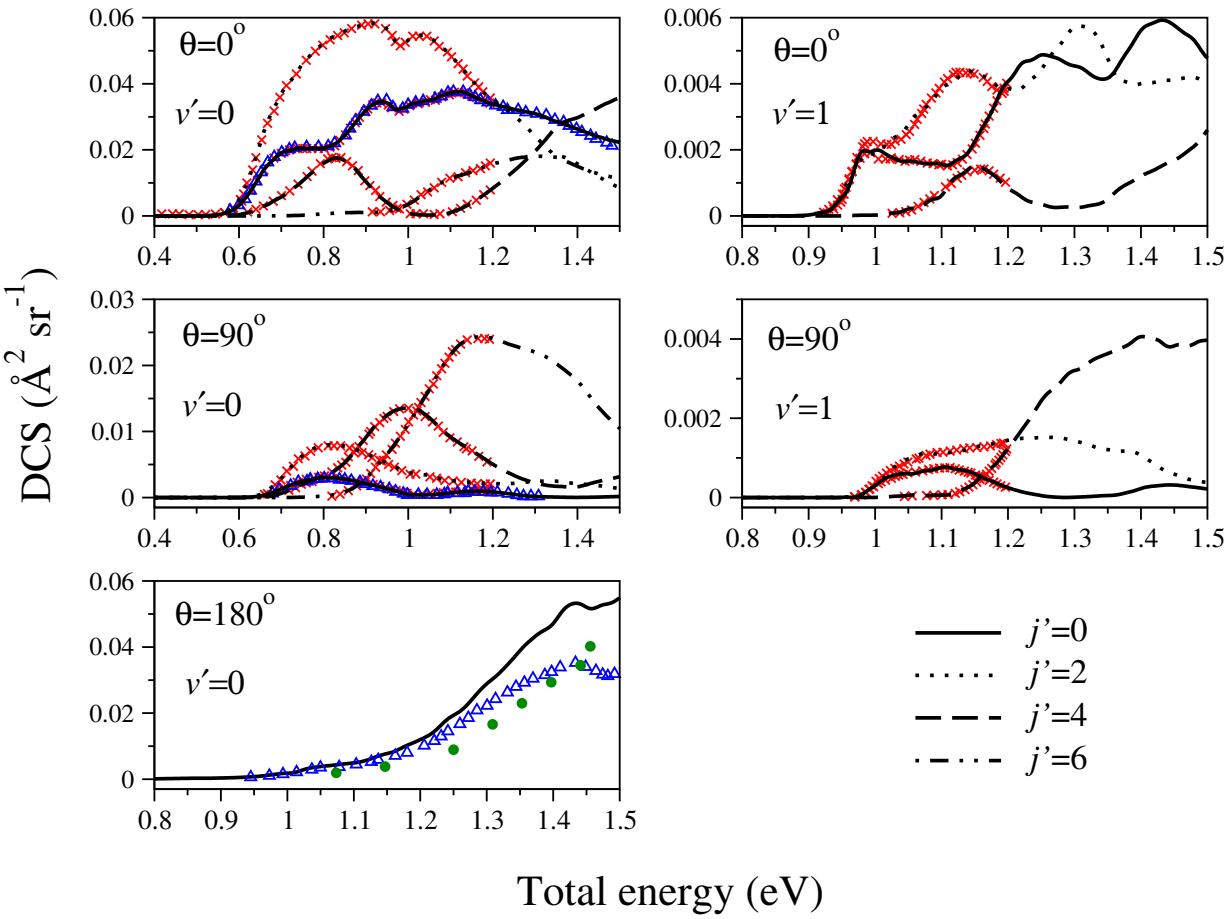

FIG. S1. Product rotational level resolved state-to-state DCSs of H + H_2 (v=0, j=0) → H_2 (v'=0-1, j'=0, 2, 4, 6) + H reaction as a function of total energy at θ = 0°, 90° and 180° calculated in the present work are compared with the results of Hankel *et al.*[1] (×), Althorpe[2] (△) and Chu *et al.*[3] (●). The results obtained from this work are shown by black curves of different types as indicated in the legend of the figure. The values of θ and v' are mentioned inside each panel.

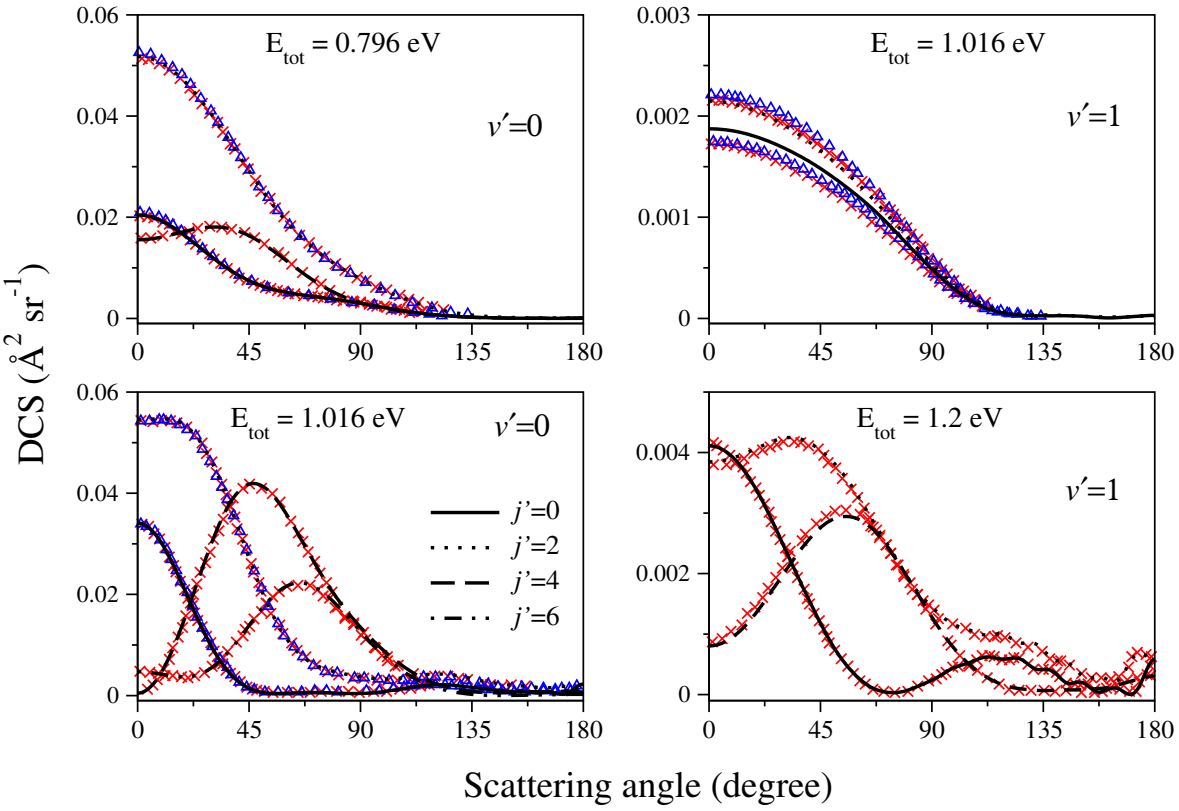

FIG. S2. Product rotational level resolved state-to-state DCSs of H + H_2 (v=0, j=0) → H_2 (v'=0-1, j'=0, 2, 4, 6) + H reaction as a function of scattering angle at various total energies, E_{tot} = 0.796 eV, 1.016 eV and 1.2 eV calculated in the present work are compared with the results of Hankel *et al.*[1] (×) and Althorpe[2] (△). The results obtained from this work are shown by black curves of different types as indicated in the legend of the figure. The values of E_{tot} and v' are mentioned inside each panel.

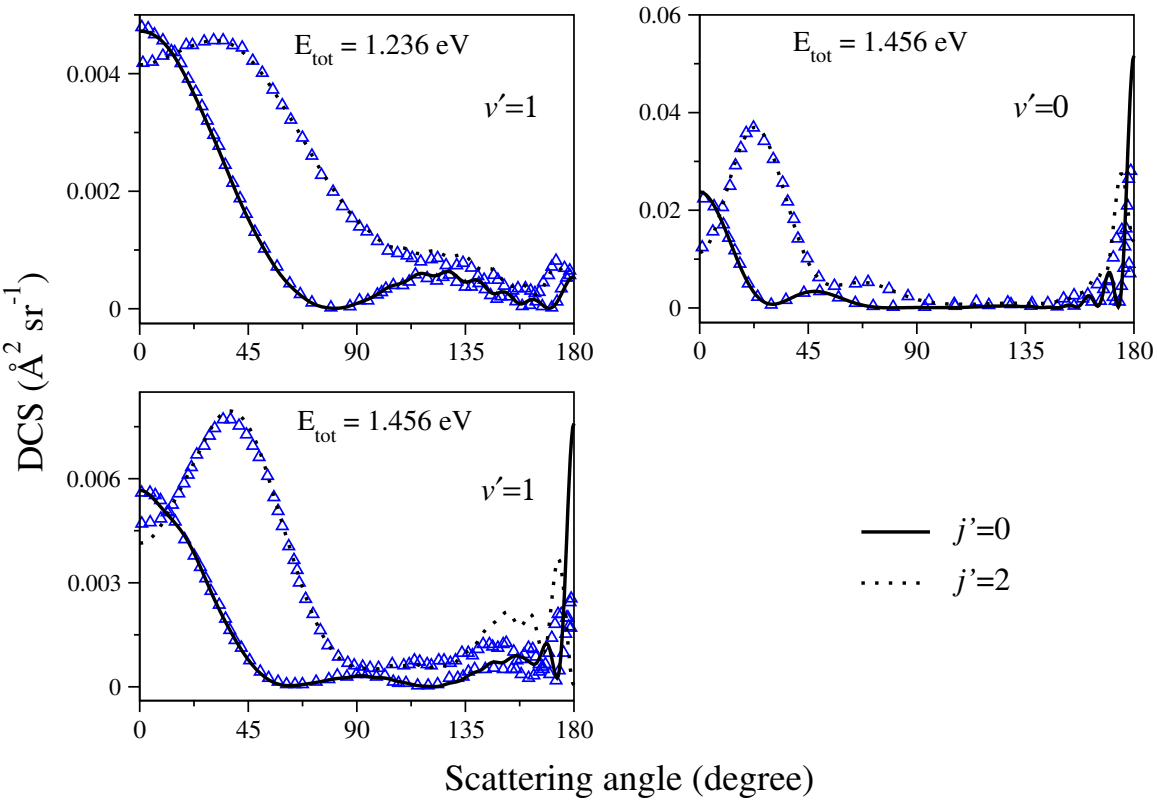

FIG. S3. Product rotational level resolved state-to-state DCSs of H + H_2 (v=0, j=0) → H_2 (v'=0-1, j'=0, 2) + H reaction as a function of scattering angle at E_{tot} = 1.236 eV and 1.456 eV calculated in the present work are compared with the results of Althorpe[2] (△). The results obtained from this work are shown by black curves of different types as indicated in the legend of the figure. The values of E_{tot} and v' are mentioned inside each panel.

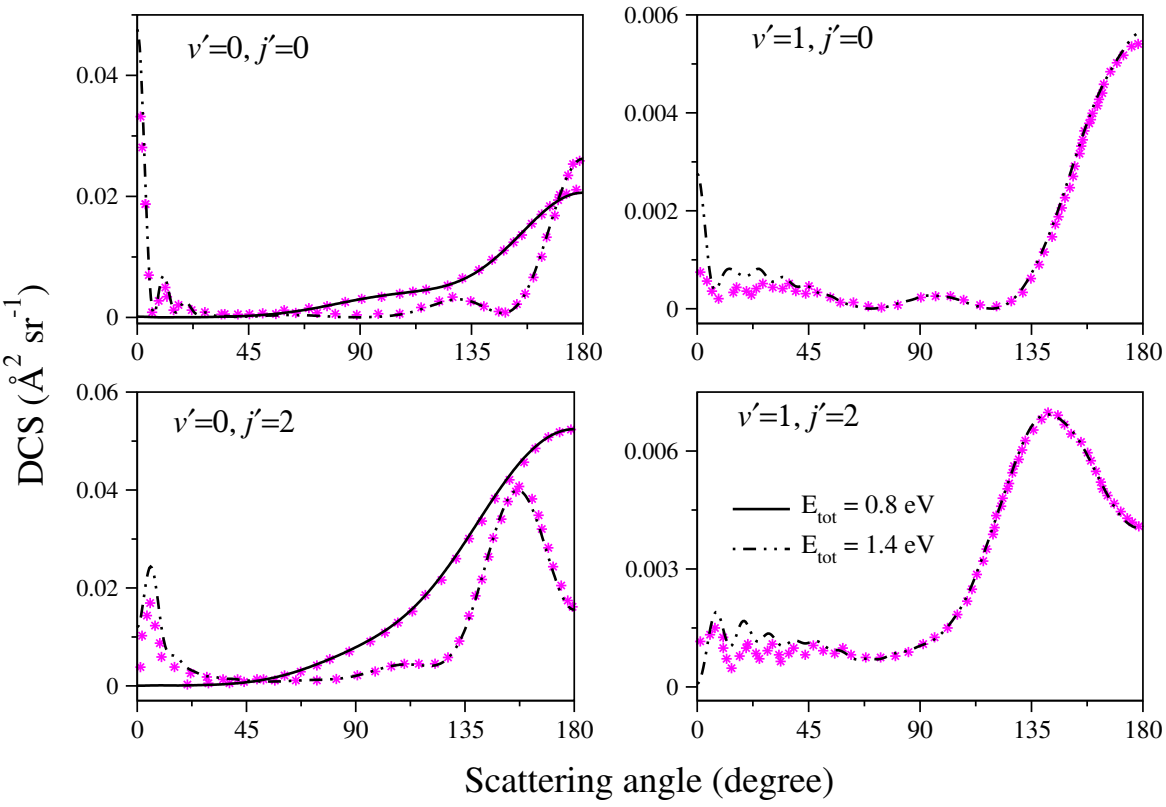

FIG. S4. Product rotational level resolved state-to-state DCSs of H + H_2 (v=0, j=0) → H_2 (v'=0-1, j'=0, 2) + H reaction as a function of scattering angle at E_{tot} = 0.8 eV and 1.4 eV calculated in the present work are compared with the results of Lin and Guo[4] (*). The results obtained from this work are shown by black curves of different types as indicated in the legend of the figure. The values of v' and j' quantum numbers are mentioned inside each panel.

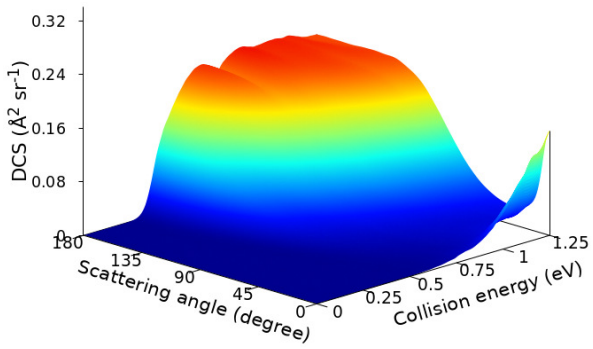

(a) H_2 (v=0, j=0)

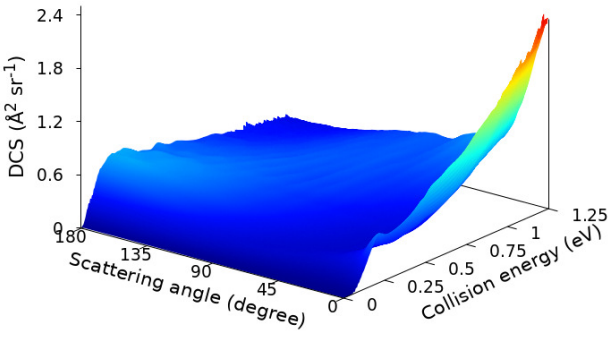

(d) H_2 (v=3, j=0)

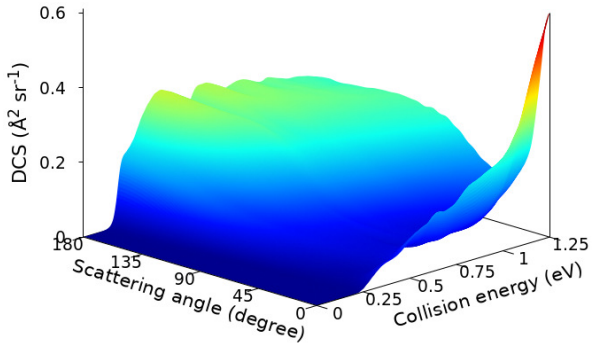

(b) H_2 (v=1, j=0)

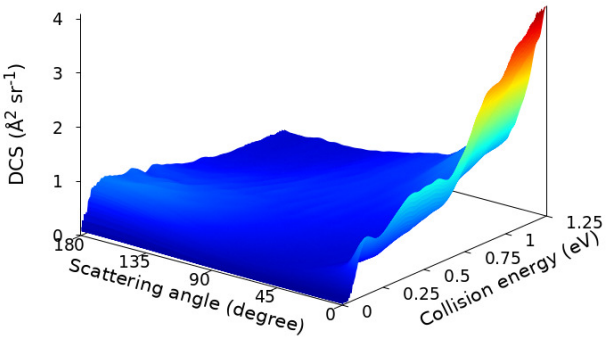

(e) H_2 (v=4, j=0)

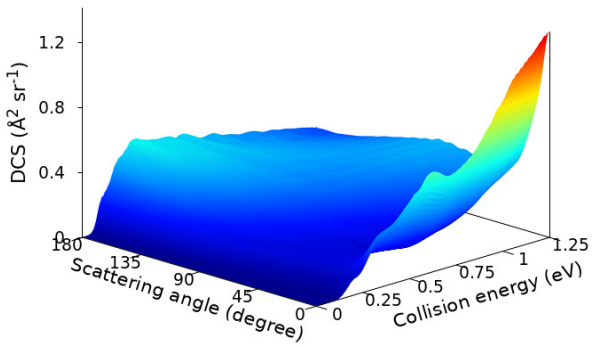

(c) H_2 (v=2, j=0)

FIG. S5. Three-dimensional perspective plot of initial state-selected total DCSs of the H + H_2 (v=0-4, j=0) → H_2 ($\sum v'$, $\sum j'$, $\sum \Omega'$) + H reaction as a function of collision energy and center-of-mass scattering angle (θ). The DCSs for reagent H_2 (v=0-2, j=0) are obtained from uncoupled surface calculations and those for H_2 (v=3-4, j=0) are obtained from coupled surface calculations.

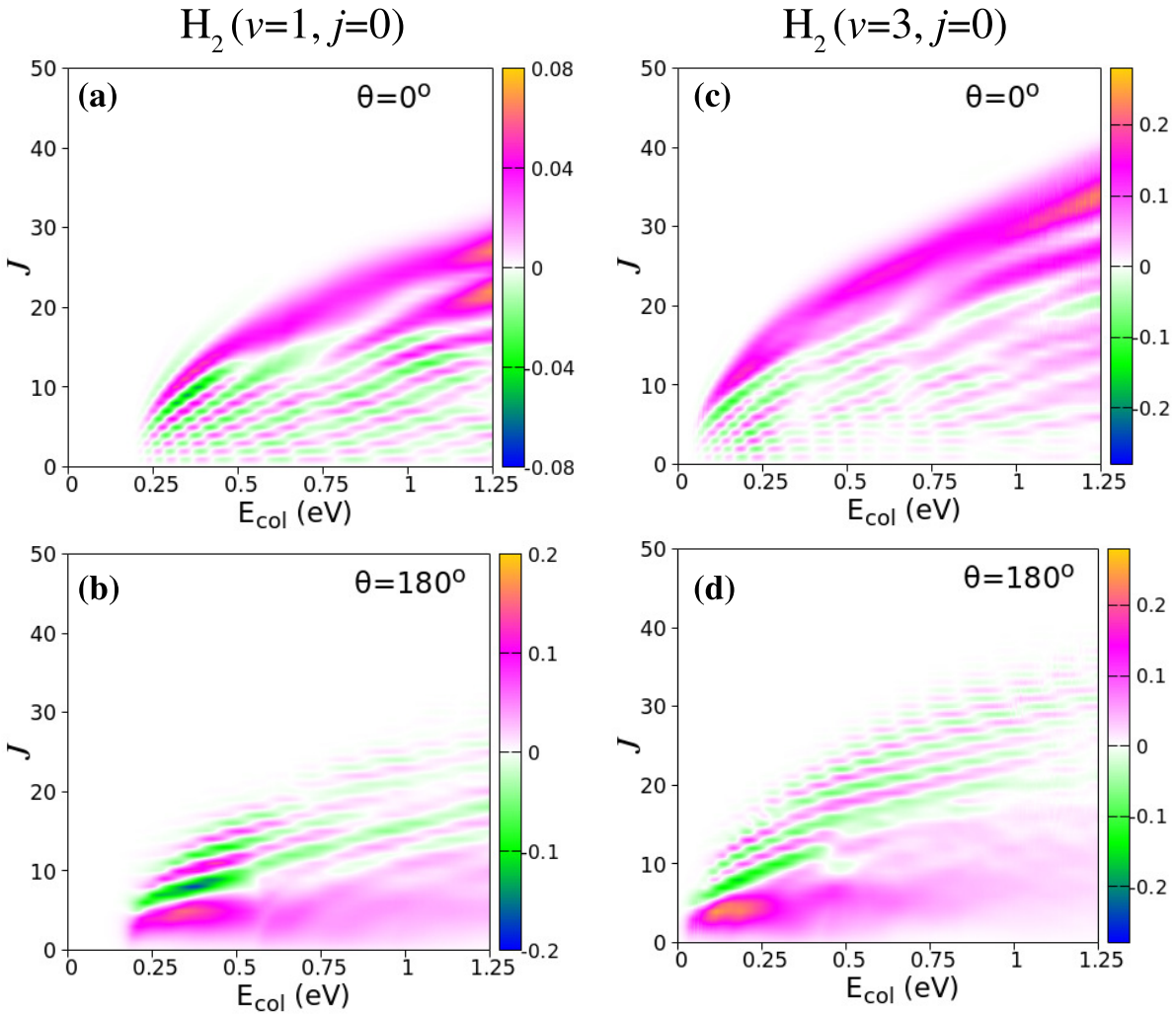

FIG. S6. Total (summed over final states) J−dependent partial DCSs (Å^2 sr^{-1}) of the H + H_2 (v=1, 3, j=0) → H_2 ($\sum v'$, $\sum j'$, $\sum \Omega'$) + H reaction shown as a function of E_{col} (abscissa) and J (ordinate) at θ = 0° (panels a and c) and 180° (panels b and d) corresponding to forward and backward scattering, respectively. The partial DCSs for reagent H_2 (v=1, j=0) are obtained from uncoupled surface calculations and that for H_2 (v=3, j=0) are obtained from coupled surface calculations.

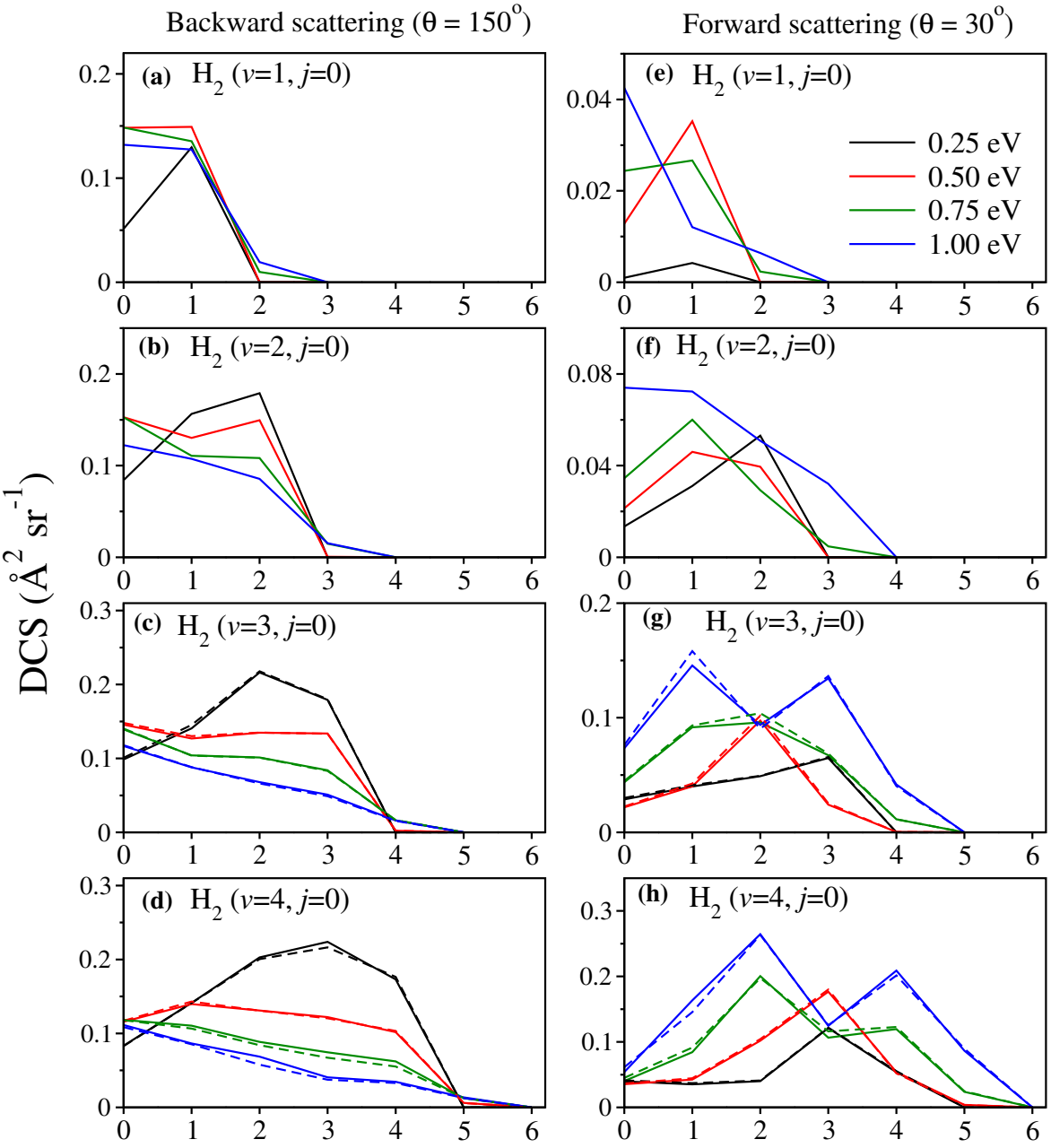

FIG. S7. Product vibrational level distributions in terms of DCS at θ = 150° (panels a-d) and 30° (panels e-h) for the H + H_2 (v=1-4, j=0) → H_2 (v', $\sum j'$, $\sum \Omega'$) + H reaction at E_{col} = 0.25, 0.50, 0.75 and 1.0 eV shown by lines of different colours. The coupled and uncoupled surface results for reagent H_2 (v=3-4, j=0) (panels c, d, g and h) are shown by solid and dashed lines, respectively, whereas the uncoupled surface results for reagent H_2 (v=1-2, j=0) (panels a, b, e and f) are shown by solid lines.

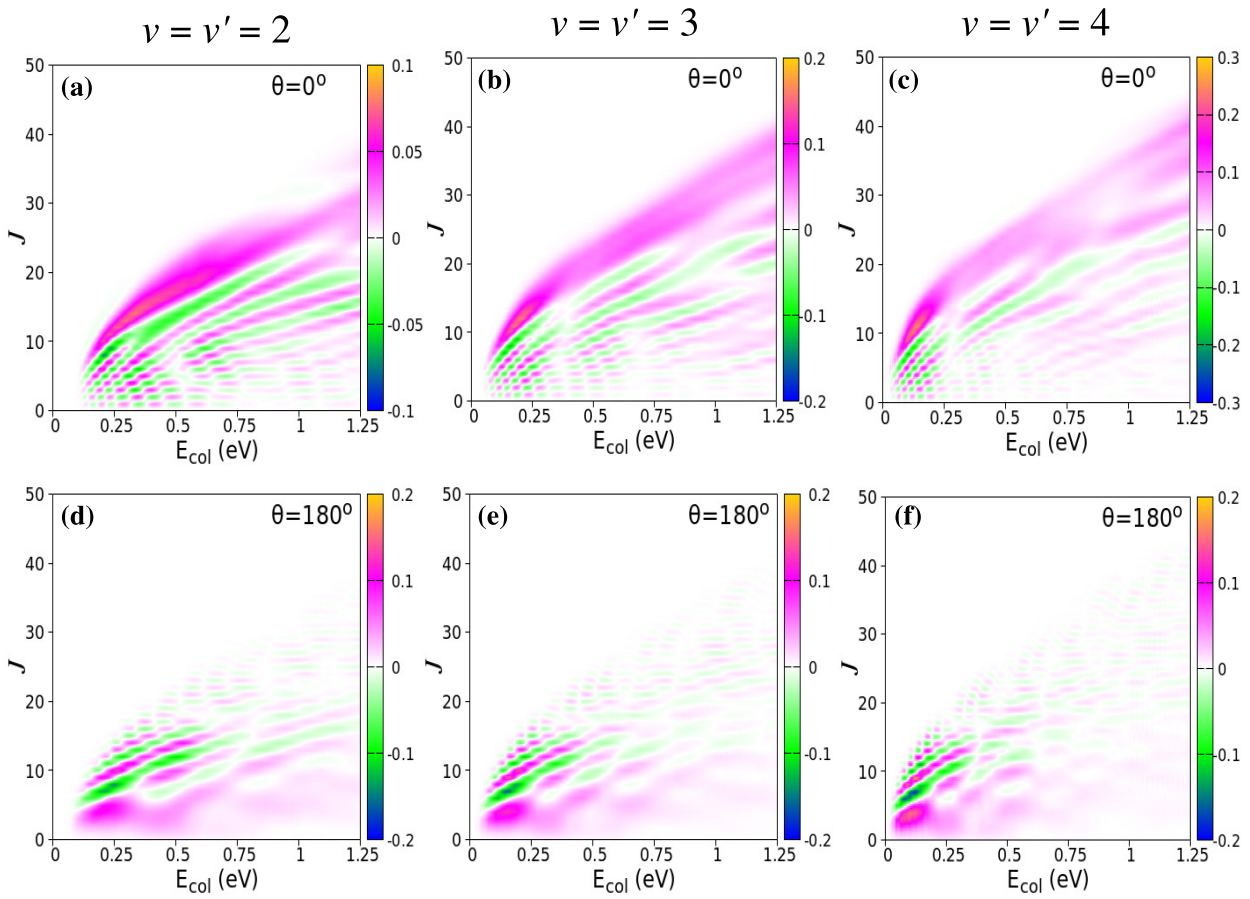

FIG. S8. Product vibrational level resolved (summed over j') J−dependent partial DCSs (Å^2 sr^{-1}) of the H + H_2 (v=2-4, j=0) → H_2 (v'=v) + H reaction shown as a function of E_{col} (abscissa) and J (ordinate) at θ = 0° (panels a-c) and 180° (panels d-f) corresponding to forward and backward scattering, respectively. The partial DCSs for reagent H_2 (v=2, j=0) are obtained from uncoupled surface calculations and those for H_2 (v=3-4, j=0) are obtained from coupled surface calculations.

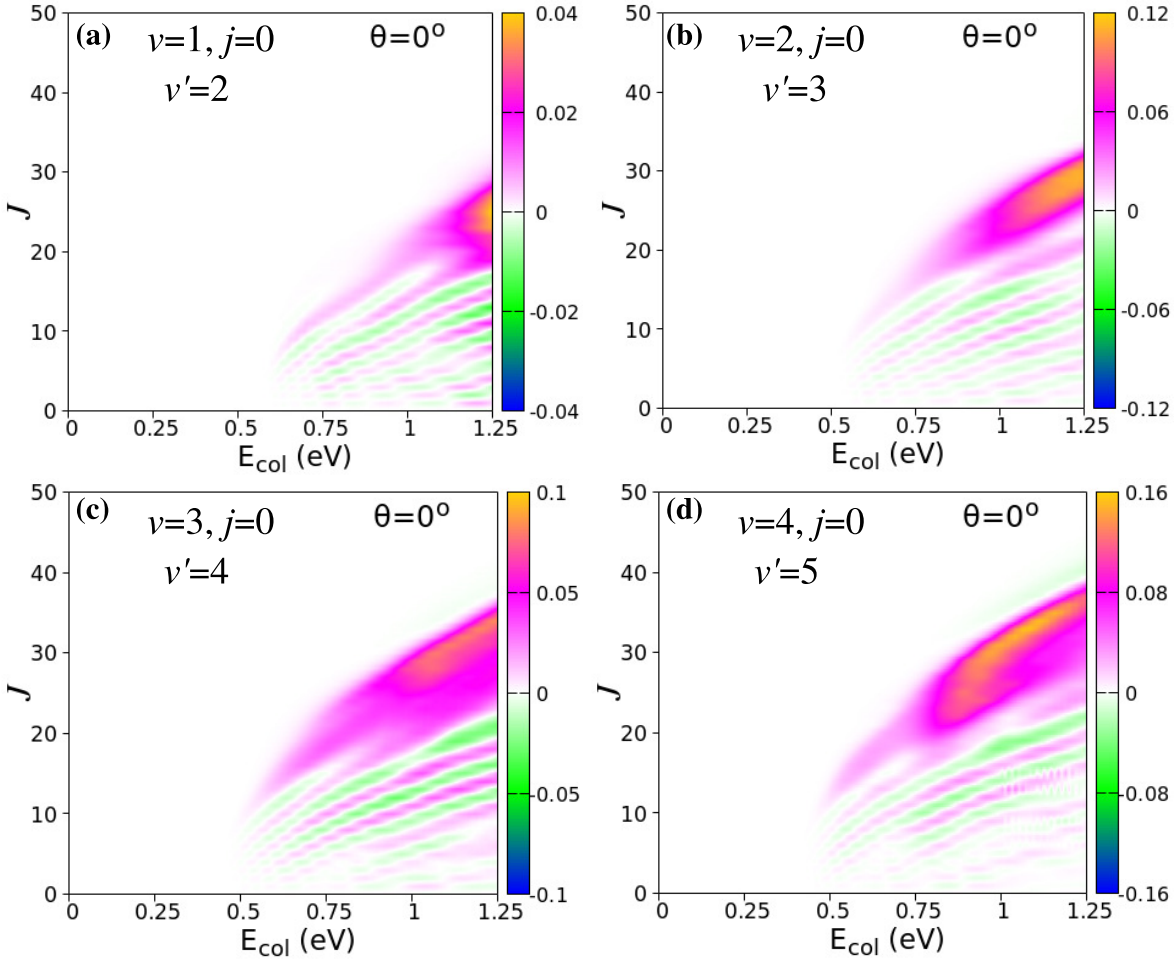

FIG. S9. Same as in Fig. S8, but for the H + H_2 (v=1-4, j=0) → H_2 (v' = v+1) + H reaction at θ = 0° corresponding to the forward scattering.

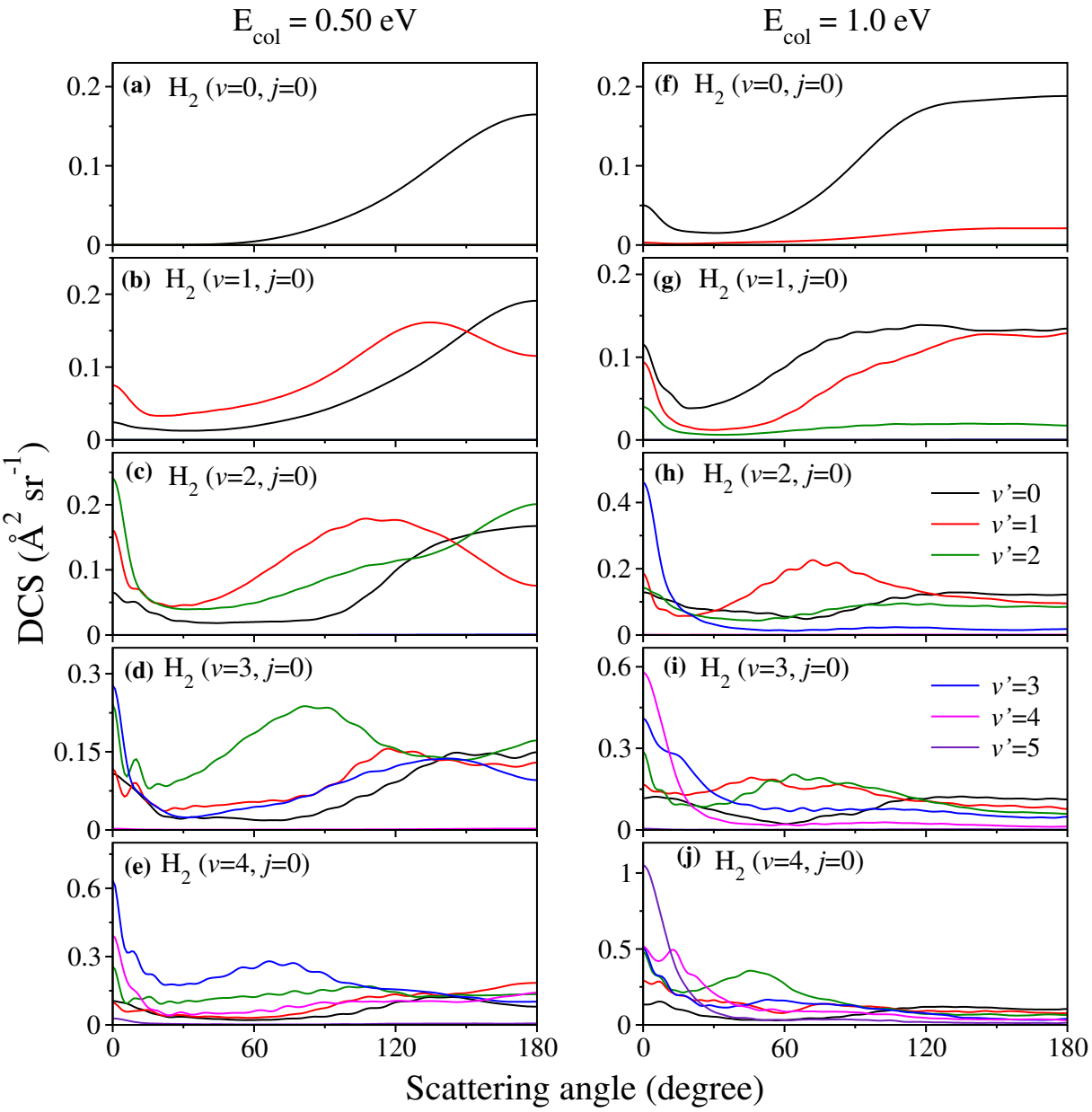

FIG. S10. Product vibrational level resolved DCSs for the H + H_2 (v=0-4, j=0) → H_2 (v', $\sum j'$, $\sum \Omega'$) + H reaction as a function of center-of-mass scattering angle (θ) at E_{col} = 0.50 and 1.25 eV shown by lines of different colours as indicated. The DCSs for reagent H_2 (v=0-2, j=0) (panels a-c and f-h) are obtained from uncoupled surface calculations and those for H_2 (v=3-4, j=0) (panels d, e, i and j) are obtained from coupled surface calculations.

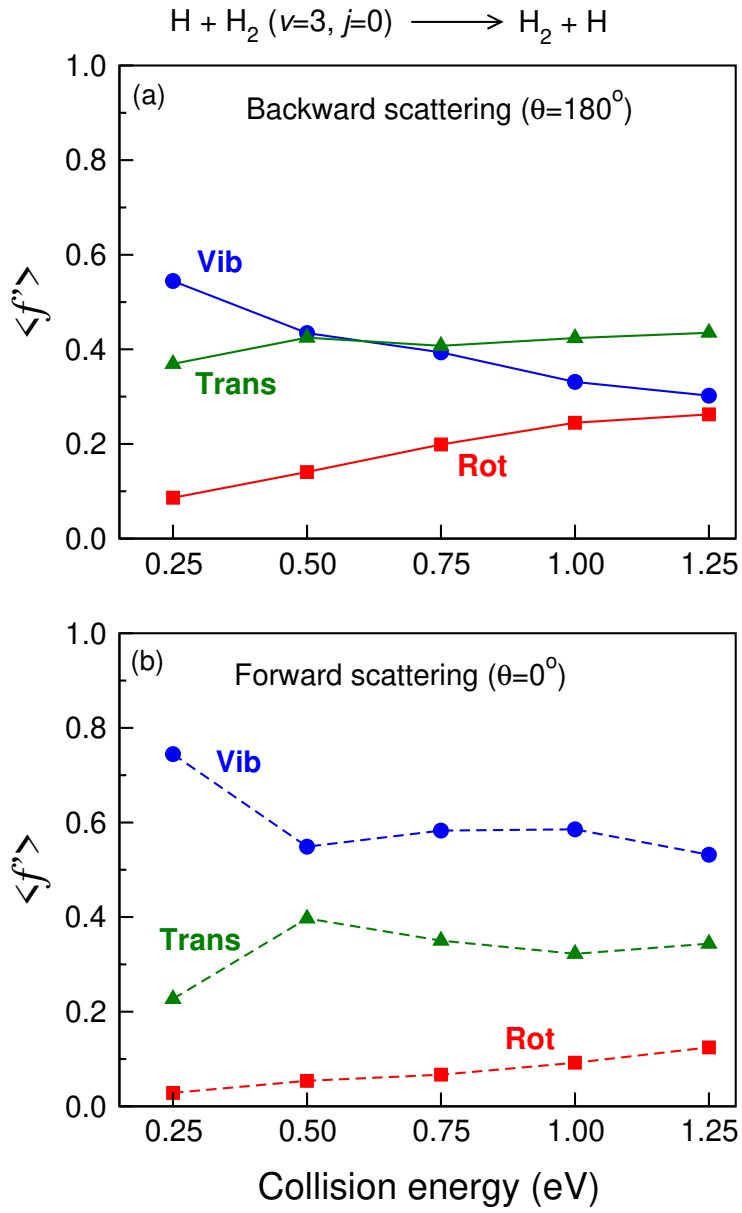

FIG. S11. Average fractions of the total available energy entering into product vibration, rotation and relative translation for the products scattered at $\theta = 180°$ (solid line) and $\theta = 0°$ (dashed line) for the H + H_2 (v=3, j=0) → H_2 + H reaction as a function of collision energy. The $\langle f' \rangle$ values are shown by lines of different colours and symbols. The abbreviations Vib, Rot and Trans represent product vibration, rotation and relative translation, respectively.

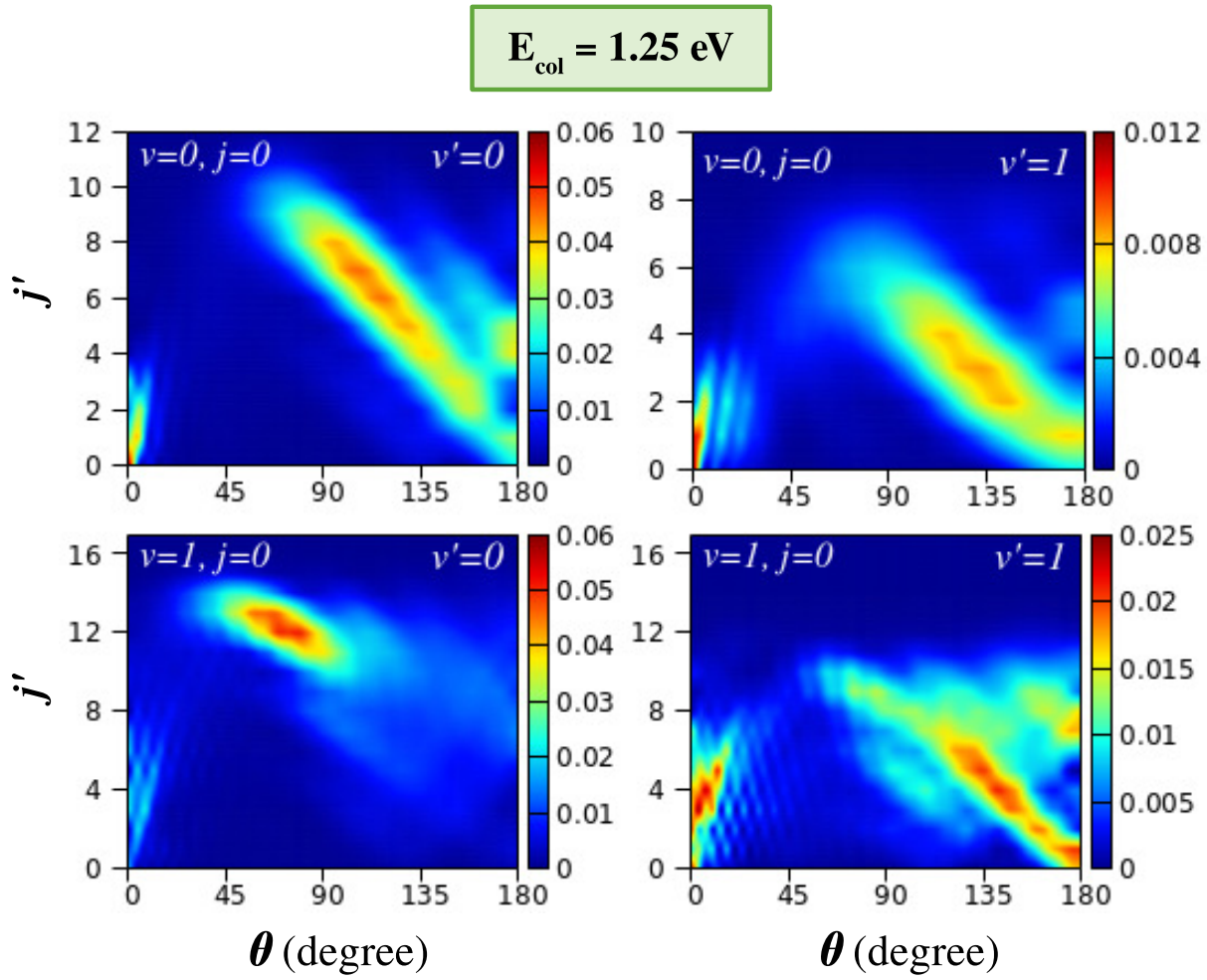

FIG. S12. Product rotational level resolved state-to-state DCSs of the H + H_2 (v=0-1, j=0) → H_2 (v'=0-1, j') + H reaction as a function of θ (abscissa) and j' (ordinate) at E_{col} = 1.25 eV.

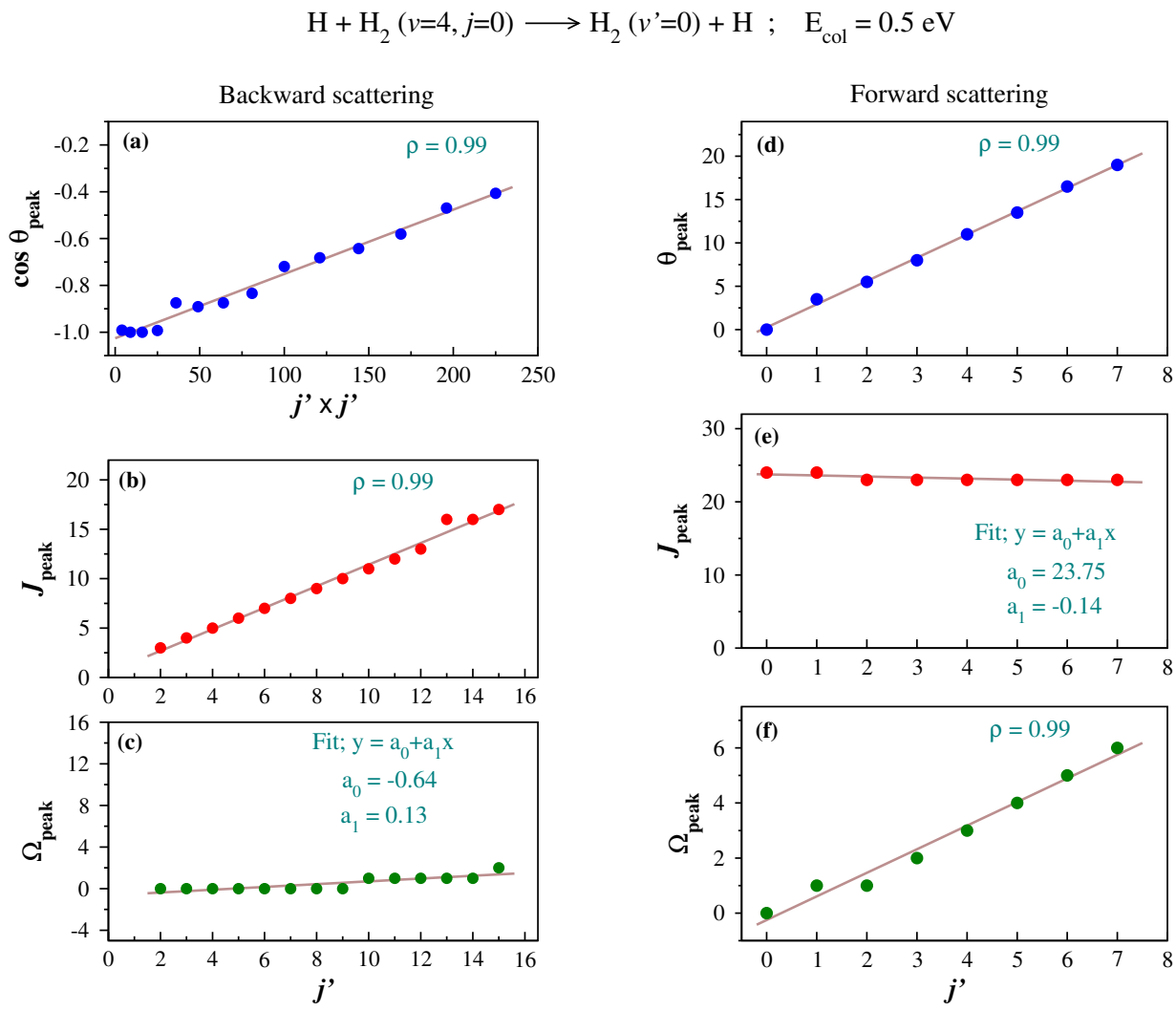

FIG. S13. Correlation among θ_{peak}, $\cos\theta_{peak}$, J_{peak}, Ω'_{peak} and j' both in the backward [(a)-(c)] and forward [(d)-(f)] scattering of the H + H_2 (v=4, j=0) → H_2 (v'=0, j') + H reaction at E_{col} = 0.5 eV. The solid lines are least-squares fit to the corresponding data by a linear equation of the type $y = a_0+a_1x$. The Pearson correlation coefficients (ρ) are mentioned inside corresponding panels to show the quality of the fit.

$H + H_2\ (v{=}4, j{=}0) \longrightarrow H_2\ (v'{=}0) + H\ ;\quad E_{col} = 0.75$ eV

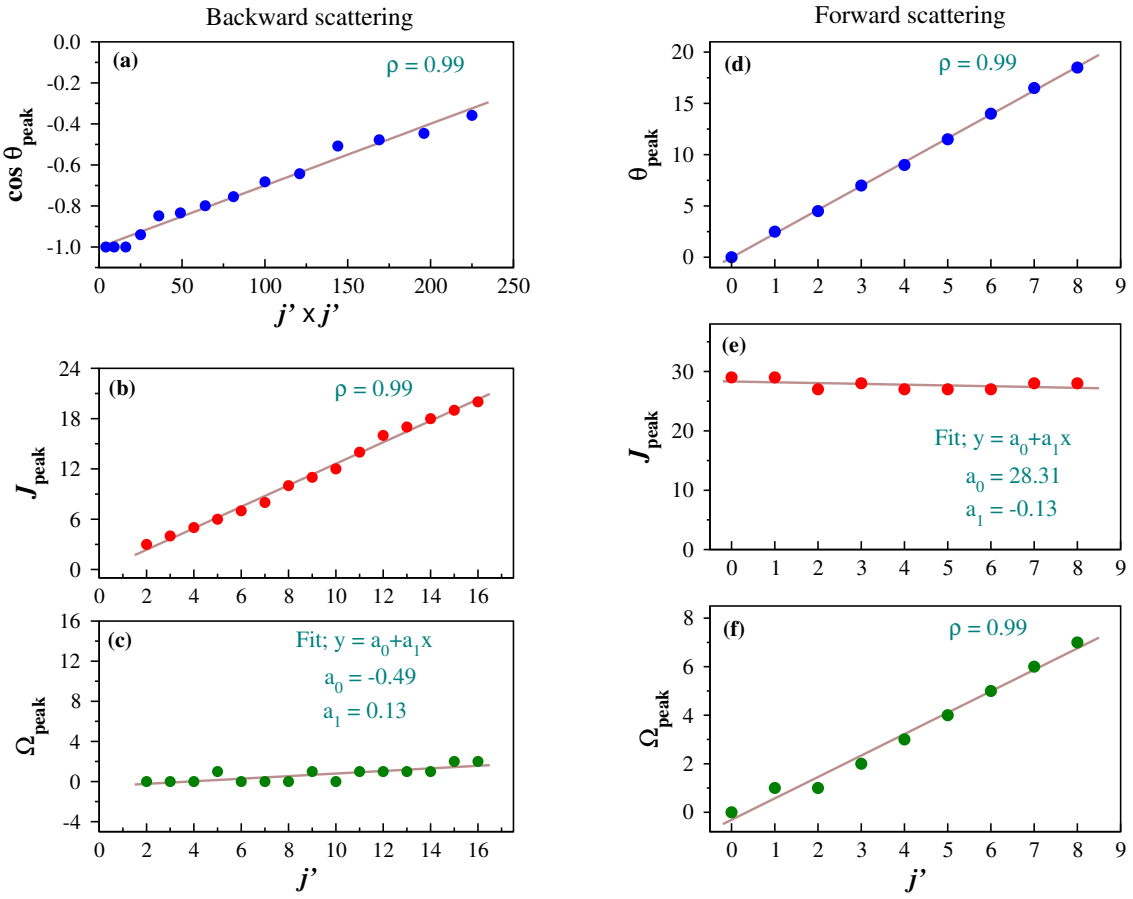

FIG. S14. Same as in Fig. S13, but at $E_{col} = 0.75$ eV.

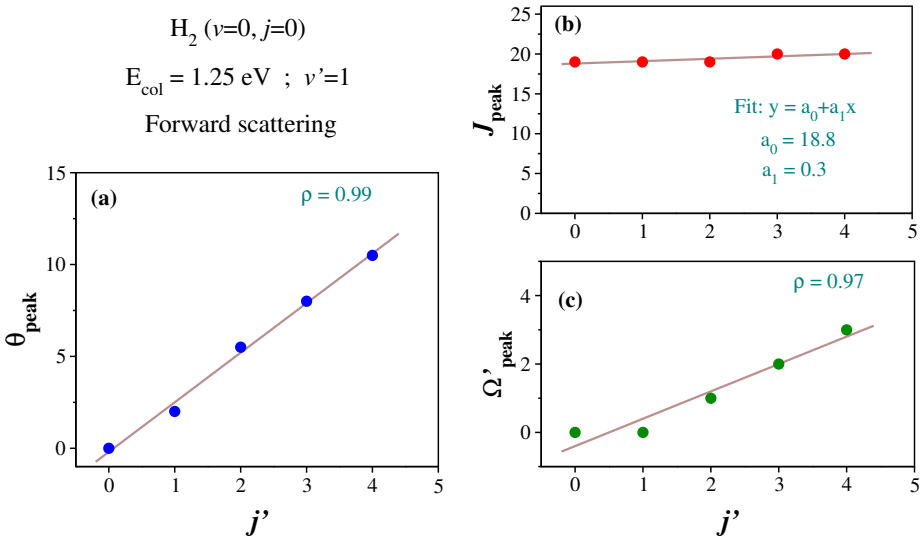

FIG. S15. Same as in Fig. S13, but for the $H + H_2\ (v{=}0,\ j{=}0) \rightarrow H_2\ (v'{=}1,\ j') + H$ reaction at $E_{col} = 1.25$ eV.

REFERENCES

[1]M. Hankel, S. C. Smith, R. J. Allan, S. K. Gray and G. G. Balint-Kurti, *J. Chem. Phys.*, 2006, **125**, 164303.

[2]S. C. Althorpe, *J. Chem. Phys.*, 2001, **114**, 1601–1616.

[3]T.-S. Chu, K.-L. Han, M. Hankel, G. G. Balint-Kurti, A. Kuppermann and R. Abrol, *J. Chem. Phys.*, 2009, **130**, 144301.

[4]S. Y. Lin and H. Guo, *Phys. Rev. A*, 2006, **74**, 022703.